ELSEVIER

Solid State Ionics 69 (1994) 265–270

SOLID STATE IONICS

Thermal stability of Li_xCoO_2, Li_xNiO_2 and λ-MnO_2 and consequences for the safety of Li-ion cells

J.R. Dahn, E.W. Fuller

Department of Physics, Simon Fraser University, Burnaby, B.C., Canada V5A 1S6

M. Obrovac, U. von Sacken

Moli Energy (1990) Ltd., 20000 Stewart Crescent, Maple Ridge, B.C., Canada V2X 9E7

Abstract

$LiCoO_2$, $LiNiO_2$ and $LiMn_2O_4$ are all stable in air to high temperatures. By contrast, Li_xCoO_2, Li_xNiO_2 and $Li_xMn_2O_4$ ($x<1$) are metastable and liberate oxygen when they are heated in air or in inert gas. The temperature at which oxygen evolution occurs depends on x and on the material. Using thermal gravimetric analysis and mass spectrometry, we have studied the thermal decomposition of these materials in inert gas. We find that the nickel materials are least stable, the manganese compounds are most stable, and that the cobalt compounds show intermediate behaviour. These results have important consequences for the safety of Li-ion cells, and suggest that cells using $LiMn_2O_4$ as the cathode should be safer than those using $LiNiO_2$ or $LiCoO_2$.

1. Introduction

Lithium-ion cells are currently the state-of-the-art in small rechargeable power sources for consumer electronics. They have the highest energy density of any commercially available rechargeable electrochemical cell. They have an operating voltage near 4 V and have been shown to have long cycle life [1–5]. Such cells use a lithium transition metal oxide (either $LiCoO_2$, $LiNiO_2$ or $LiMn_2O_4$) as the positive electrode and a form of carbon or graphite as the negative electrode.

Lithium-ion cells of small size have been demonstrated to be safe in consumer applications. Some researchers are even proposing that the Li-ion chemistry is suitable for large cells, such as those for electric vehicles. However, it must be noted that the safety of the small consumer cells has only been achieved with carefully designed cell safety features. For example, the $LiCoO_2$/carbon cell produced by Sony Energytec has a pressure activated disconnect to prevent overcharge of the cell [6]. As the cells are charged above 4.2 V, pressure is generated by the decomposition of electrolyte and cathode additives to the cell [7]. Once the pressure reaches a critical value, the disconnect activates and prevents current flow to the cell. Why is such a feature necessary? In earlier work on $LiNiO_2$/carbon coin cells, we learned that such cells could be made to vent violently if a spot welder pulse were applied to the positive (lithium nickel oxide) cell case after the cells were charged to create $Li_{0.3}NiO_2$ [8]. We reported that $Li_{0.3}NiO_2$ is unstable at high temperatures and can liberate oxygen into an electrolyte heated above its flash point, leading to a violent reaction. The amount of oxygen released on heating increases as x decreases in Li_xNiO_2, so it is important to keep x from getting too small. It is our opinion that a pressure disconnect is required

Elsevier Science B.V.
SSDI 0167-2738(94)00067-3

to prevent x in Li_xCoO_2 from decreasing substantially below 0.5 for the same reason. Furthermore, it has been shown that the reversibility of Li_xCoO_2 is good for $0.4<x<1$, but that it degrades rapidly for $x<0.3$ (See Fig. 2b in Ref. [9]). This could also be caused by the instability of Li_xCoO_2 to oxygen release.

Other workers have noticed the sensitivity of Li_xNiO_2 and Li_xCoO_2 to heating. Recently, Wainwright [10] completed a study of the behaviour of Li_xNiO_2/carbon and Li_xCoO_2/carbon coin cells exposed to spot welder pulses on the positive electrode cell case. He showed that the welder power needed to initiate cell venting decreased significantly as x in Li_xMO_2 (M=Ni, Co) decreased. This was caused by a decrease in the stability of these materials to oxygen loss on heating, as x is decreased. There is no doubt that the oxygen release from these materials constitutes a problem that must be addressed to make cells abuse-tolerant. The appearance of recent patent applications [11] describing means of improving the safety of $LiCoO_2$/carbon cells in overcharge situations further underscores the importance of understanding the thermal decomposition of Li_xMO_2 compounds.

In a recent work, Morales et al. [12] studied the thermal behaviour of $Li_{x-y}Ni_{2-x}O_2$ samples made initially from $Li_xNi_{2-x}O_2$ where x was 0.77. Values of y ranged from 0 to 0.5. For $y<0.4$, the materials decomposed, liberating oxygen, above 400°C. For $0.4<y<0.5$, a significant weight loss was seen near 250°C. This was associated [12] with the release of oxygen necessary for the formation of a spinel phase related to $LiNi_2O_4$ [13]. For $y<0.4$ in these samples no oxygen release near 250°C is required to form the spinel phase. Above 400°C, all samples of $Li_{x-y}Ni_{2-x}O_2$ were thought to undergo the following reaction:

$$Li_{x-y}Ni_{2-x}O_2 \Rightarrow Li_{x-y}Ni_{2-x}O_{2-y} + (y/2)O_2 . \quad (1)$$

$Li_{x-y}Ni_{2-x}O_{2-y}$ is a member of the rock-salt-related solid solution $Li_zNi_{2-z}O_2$, which has equal numbers of cations and anions. The crystal structure of this solid solution series has been carefully studied as a function of z [14,15].

It is difficult to apply the results of [12] directly to the safety of Li-ion cell cathode materials, because those are generally made as stoichiometric as possible. $Li_{0.77}Ni_{1.23}O_2$ (used in the Morales et al. [13] study) has substantial amounts of nickel atoms in the layers normally only occupied by lithium in $LiNiO_2$ [14,15]. These misplaced nickel atoms significantly reduce the specific capacity of the electrode material over that of approximately stoichiometric $LiNiO_2$ [8] and such materials are therefore not generally used in practical or prototype cells. It is also likely that the thermal behavior of $Li_{1-y}NiO_2$ will be significantly different from that of $Li_{0.77-y}Ni_{1.23}O_2$.

Here, we describe the thermal behaviour of Li_xNiO_2, Li_xCoO_2 and λ-MnO_2. λ-MnO_2 is made by removing almost all of the lithium from $LiMn_2O_4$. Each of these materials evolves oxygen upon heating in inert gas. We discuss the implications of the results on the safety of Li-ion cells.

2. Experimental

$LiNiO_2$ was made by reacting NiO and $LiOH \cdot H_2O$ at 700°C as described in Ref. [16]. $LiCoO_2$ was prepared from Li_2CO_3 and Co_3O_4. $LiMn_2O_4$ was prepared by reacting MnO_2 (Electrolytic Manganese Dioxide, Chemetals, Baltimore, Md., USA) and Li_2CO_3 at 750°C. The lattice constants of these starting materials are given in Table 1.

Li_xNiO_2 and Li_xCoO_2 were prepared electrochemically using the hardware described in [17]. First, a stainless steel wire mesh (80 wires per inch) was placed in the bottom of the cell container. Then two pieces of Celgard 2502 microporous film were placed on top of the mesh and a polypropylene sleeve insulator was pushed down on the separator. Then, 0.10 g of a mixture of the starting material with 5% carbon black (Ensagri Super S) was carefully added on top of the separator, within the sleeve. The active ingredients and the separator were then wetted with 1M $LiPF_6$ dissolved in a 50/50 mixture of PC (propylene carbonate) and DME (dimethoxyethane). An

Table 1
Lattice constants of the starting materials

Material	a(Å)	c (Å)
$LiNiO_2$	2.878	14.18
$LiCoO_2$	2.817	14.05
$LiMn_2O_4$	8.240	cubic

aluminum contact plate was then inserted into the sleeve and pressed against the active powder layer by a spring. The compressed spring applied a pressure of about 15 bar to the cell stack. No metallic Li is included in the cell as constructed, but once the cell is started on charge, metallic Li is electroplated within the holes of the wire mesh and then the cell voltage can be used to monitor the lithium concentration in the electrode by comparing to previously measured voltage-composition ($V(x)$) curves ([9] for $Li_x CoO_2$ and [18] for $LiNiO_2$). Cells were typically charged at 0.25 mA to the voltage corresponding to the desired x, and then equilibrated at that voltage for about 10 h. For example, $Li_{0.4}CoO_2$ and $Li_{0.3}NiO_2$ were prepared by charging to 4.4 and 4.2 V respectively.

After equilibration, the cells were disassembled in a helium filled glove box and the active electrode powder recovered. The plated Li deposit in the stainless steel mesh was used to check the uniformity of the sample. Only when uniform Li deposits were found, were the samples used. The recovered cathode powder was then rinsed with DME, vacuum dried and stored under argon. The use of elastomeric binders in the cathode was rigorously avoided because we have observed spurious mass losses on heating of these samples in cases where binders were used.

λ-MnO_2 was prepared using the methods of Ref. [19]. 10 g of $LiMn_2O_4$ was stirred in aqueous HCl solution (pH = 1) at 90°C for about 30 min. The material was then filtered, rinsed with water and vacuum dried at 50°C. The lattice constant of the product was 8.05 Å, in good agreement with literature values for λ-MnO_2.

A TA instruments model 951 Thermal Gravimetric Analyzer (TGA) was used for the thermal stability experiments. For some experiments, the gaseous products of thermal decomposition were passed to a Leybold Quadrex 100 mass spectrometer, equipped with an atmospheric pressure inlet system. Using the mass spectrometer, we were able to identify the gases evolved. All TGA experiments were made under inert gas, either helium or argon. Scan rates ranged from 0.25°C/min to 25°C/min. Some of the TGA products were analyzed by powder X-ray diffraction.

3. Results

In general, weight losses measured with the TGA were found to be almost entirely due to loss of oxygen. Thus, weight loss readings from the TGA can be interpreted as the weight of oxygen lost by the sample. The only other weight losses were small. There is some desorption of CO_2 from the Li_xNiO_2 and Li_xCoO_2 samples below 400°C and some combustion of carbon black above 450°C. For the λ-MnO_2 sample, there is some release of water near 150°C, probably due to incorporated H atoms from the acid treatment process. Upon heating, these H atoms react with oxygen atoms in the MnO_2, producing water.

Fig. 1 shows TGA results for $Li_{0.3}NiO_2$ measured at four different heating rates. There are significant changes to the weight loss profile as the heating rate is changed. This is shown more clearly when dM/dT (derivative of sample weight versus temperature) is plotted versus the sample temperature, as in Fig. 2 for two of the four heating rates. Each of the peaks in Fig. 2 is due to the loss of oxygen from the sample. Numerous peaks can be resolved in the derivative of the slow (0.5°C/min) scan, which points to a very complex decomposition process, involving the formation of several intermediate phases. Note that at low heating rates this material decomposes well below 200°C.

Fig. 3 shows the TGA results for a series of Li_xNiO_2 samples with $x = 0.5$, 0.4 and 0.3 respectively, all measured at a sweep rate of 20°C/min. The large

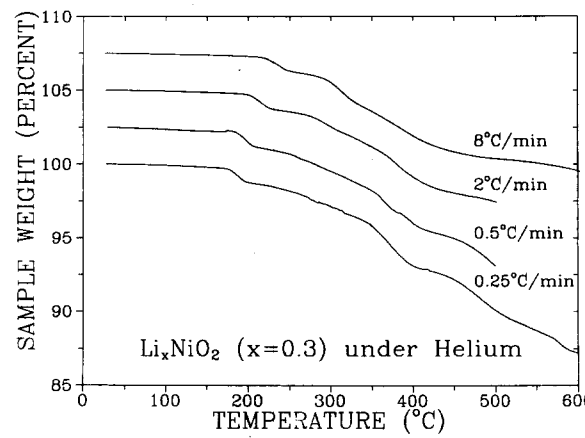

Fig. 1. TGA results for $Li_{0.3}NiO_2$ under helium at the four heating rates indicated. The data have been offset vertically by 2.5% sequentially for clarity.

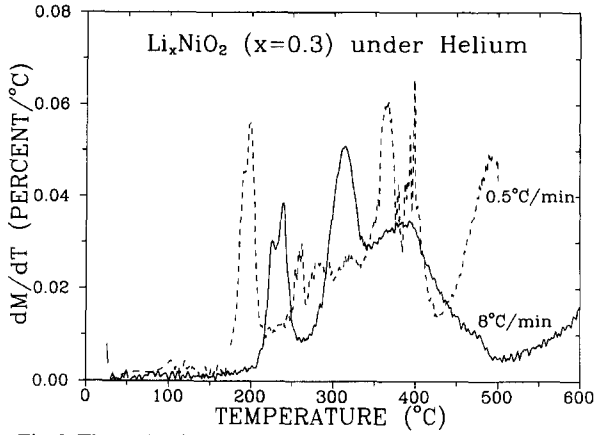

Fig. 2. The derivative, dM/dT, versus temperature for two of the data sets shown in Fig. 1.

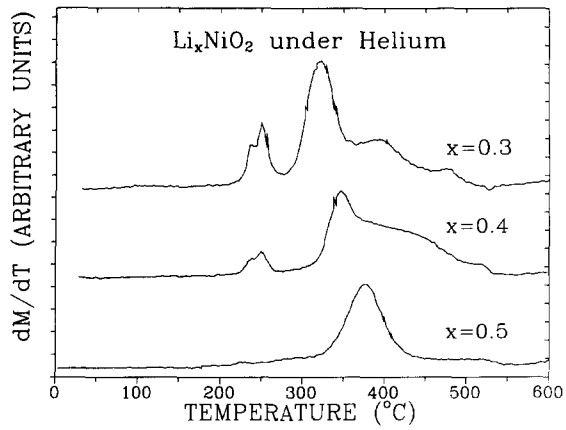

Fig. 3. The derivative, dM/dT, versus temperature calculated from TGA measurements on samples of Li_xNiO_2 with $x=0.3$, 0.4, and 0.5, as indicated. The data has been offset vertically for clarity.

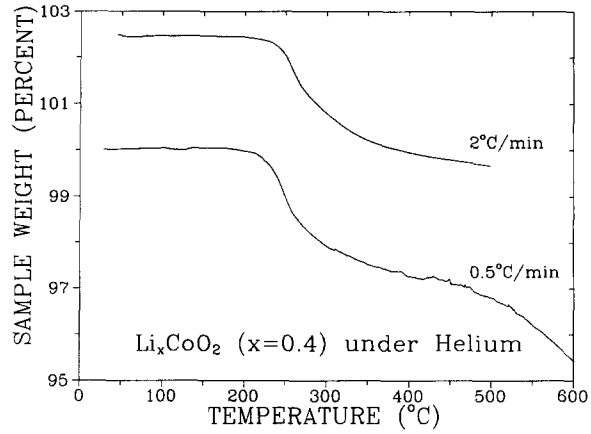

Fig. 4. TGA results for $Li_{0.4}CoO_2$ under helium at the two heating rates indicated. The data have been offset vertically by 2.5% sequentially for clarity.

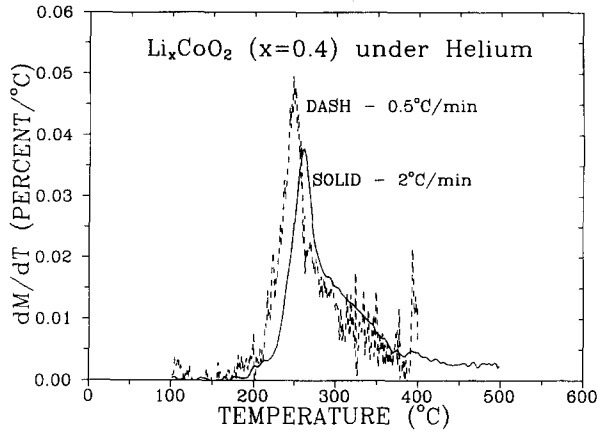

Fig. 5. The derivative, dM/dT, versus temperature for the two data sets shown in Fig. 4.

peak near 230°C shrinks as x increases and is absent for $x=0.5$. It is well known that $Li_{0.5}NiO_2$ converts to spinel $LiNi_2O_4$ near 200°C [13]. For the $x=0.5$ sample, no weight loss is involved. For $x<0.5$, the conversion to spinel is apparently accompanied by oxygen release, because there are more than 4 oxygen atoms for 3 cations in such samples. At higher temperatures Li_xNiO_2 then converts to members of the series $Li_xNi_{2-x}O_2$ with further weight loss in a complex process. Further work is needed to understand the details of this conversion. Notice that the main peak in Fig. 3 shifts to lower T as x decreases.

Fig. 4 shows the results of TGA measurements on $Li_{0.4}CoO_2$. The large weight loss near 250°C occurs in what appears to be a single event. Fig. 5 shows the derivative, dM/dT, for the data of Fig. 4. Examination of the heated product by X-ray diffraction after the 2°C/min heating showed $LiCoO_2$ and Co_3O_4, consistent with the reaction:

$$Li_xCoO_2 \Rightarrow (1-x)/3\ Co_3O_4 + xLiCoO_2 + (1-x)/3\ O_2\,. \quad (2)$$

However, the weight loss observed is substantially less than predicted by Eq. (2), so the Co_3O_4 may be non-stoichiometric. All the Li_xCoO_2 samples studied for $0.4<x<0.6$ showed the same behavior. All showed weight loss beginning near 220°C and all gave products of $LiCoO_2$ and Co_3O_4.

Fig. 6 shows the TGA results for λ-MnO_2 heated in argon at two rates and Fig. 7 shows dM/dT versus T for the same two experiments. The small weight loss near 150°C was caused by water, as confirmed by the mass spectrometer. Only when the sample temperature exceeded about 300°C, were we able to detect oxygen evolution. The water evolved near 150°C is most likely produced by the reaction of incorporated hydrogen (from the acid treatment to prepare λ-MnO_2) with lattice oxygen. The weight loss to 500°C in Fig. 6 is consistent with the reaction:

$$\lambda\text{-}MnO_2 \Rightarrow \tfrac{1}{2}Mn_2O_3 + \tfrac{1}{4}O_2 . \quad (3)$$

Tarascon and Guyomard [20] studied the thermal stability of λ-MnO_2 in air. They found that significant oxygen release did not occur until over 400°C, in basic agreement with the results in Figs. 6 and 7. As expected, the oxygen release from λ-MnO_2 starts at lower temperatures in argon than in air.

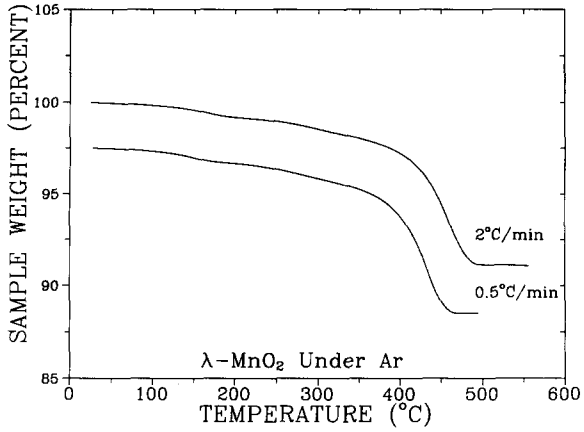

Fig. 6. TGA results for λ-MnO_2 under argon at the two heating rates indicated. The data have been offset vertically by 2.5% sequentially for clarity.

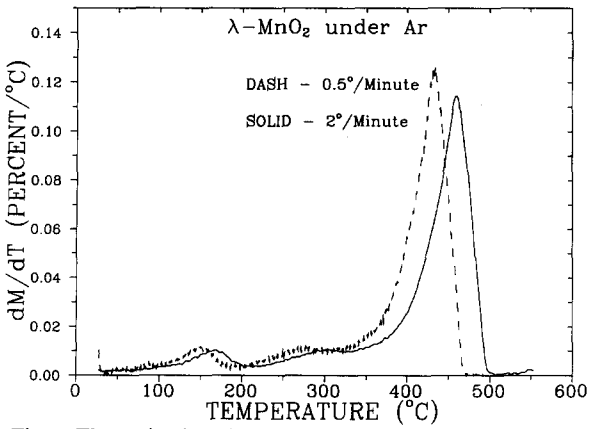

Fig. 7. The derivative, dM/dT, versus temperature for the two data sets shown in Fig. 6.

Fig. 8 compares the oxygen release onset temperatures for $Li_{0.3}NiO_2$, $Li_{0.4}CoO_2$ and λ-MnO_2 as a function of heating rate. We have taken the onset temperature to be that point where $dM/dT = -0.02\%/°C$. These stoichiometries correspond to the minimum amount of lithium incorporated to ensure good electrochemical reversibility (i.e. typical fully charged state of these materials). That is, it is unlikely that lower values of lithium content would be encountered in a practical Li-ion cell incorporating any of these cathodes. Fig. 8 shows that oxygen release from λ-MnO_2 occurs at much higher temperatures than from the other materials. Therefore, we expect Li-ion cells using $LiMn_2O_4$ cathodes to be much more tolerant of electrical and thermal abuse than those with $LiNiO_2$ or $LiCoO_2$ cathodes. For completeness, Fig. 9 compares dM/dT versus T for the 3 electrode materials measured at a heating rate of 2°C/min. This again shows the increased stability of λ-MnO_2 compared to $Li_{0.3}NiO_2$ and $Li_{0.4}CoO_2$.

The results in Fig. 8 show that oxygen evolution from, for example, Li_xNiO_2 occurs slowly at temperatures near 150°C. If we extrapolate the line in Fig. 8 which passes through the data for the nickel compound to lower heating rates, we can estimate the lifetime of $Li_{0.3}NiO_2$ at lower temperatures. We assume that the lifetime at a particular temperature is approximately the inverse of the heating rate where

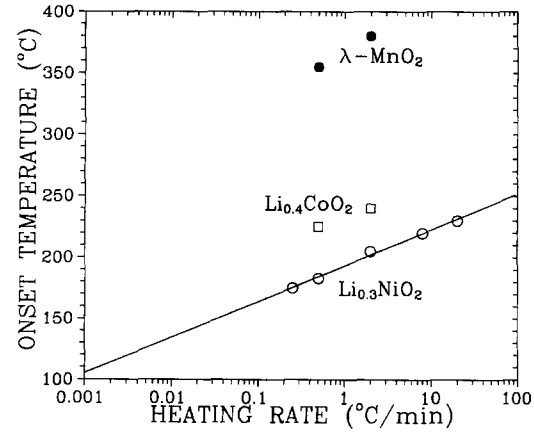

Fig. 8. The onset temperature for oxygen release for $Li_{0.3}NiO_2$, $Li_{0.4}CoO_2$ and λ-MnO_2 as a function of sample heating rate.

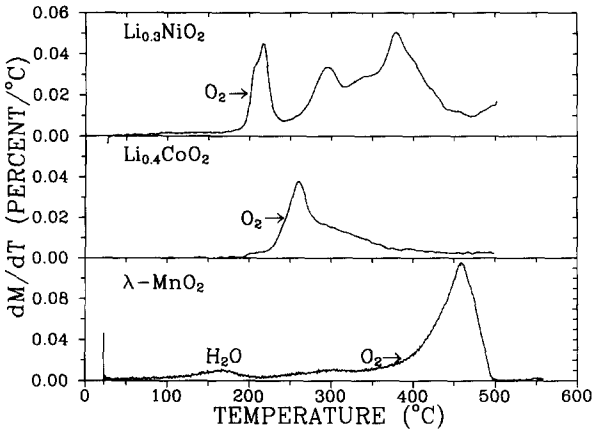

Fig. 9. Comparing the derivative, dM/dT, versus temperature for $Li_{0.3}NiO_2$, $Li_{0.4}CoO_2$ and λ-MnO_2. Each data set was measured at a heating rate of 2°C/min under inert gas. The oxygen release onsets used in Fig. 8 are indicated in each graph. The first peak in the λ-MnO_2 data is due to H_2O release.

oxygen evolution will be seen at the same temperature. The predicted lifetime at 100°C is then the order of days for $Li_{0.3}NiO_2$, assuming the extrapolation is valid. This suggests that it will be difficult to make cells based on $LiCoO_2$ or $LiNiO_2$ which operate well at high temperatures. Tarascon and Guyomard [20] showed that although λ-MnO_2 does not evolve oxygen until near 400°C, it transforms to other phases of MnO_2 upon heating. For example, near 190°C, λ-MnO_2 transforms to ε-MnO_2 which is believed to be electrochemically inactive. Therefore, it may also be difficult to operate cells using $LiMn_2O_4$ at elevated temperatures.

4. Conclusions

The TGA experiments described here show that each of Li_xNiO_2, Li_xCoO_2 and λ-MnO_2 liberate oxygen upon heating. The onset temperature for oxygen evolution is highest for λ-MnO_2. It is not desirable to have large amounts of oxygen liberated into Li-ion cells under abusive conditions, so it is important to minimize the rate at which oxygen can be generated. This can be accomplished by using $LiMn_2O_4$ instead of $LiNiO_2$ or $LiCoO_2$ as the cathode for Li-ion cells.

References

[1] K. Sekai, H. Azuma, A. Omaru, S. Fujita, H. Imoto, T. Endo, K. Yamamura and Y. Nishi, J. Power Sources 43 (1993) 241.
[2] T. Nagaura and K. Tozawa, Prog. Batteries Solar Cells 9 (1990) 209.
[3] J.R. Dahn, U. von Sacken, M.W. Juzkow and H. Al-Janaby, J. Electrochem. Soc. 138 (1991) 2207.
[4] I. Kuribayashi, J.E.E., J. Electron. Eng. 30 (1993) 51.
[5] J. Yamamura, Y. Ozaki, A. Morita and A. Ohta, J. Power Sources 43 (1993) 233.
[6] Y. Oishi, T. Abe, T. Nagaura and M. Watanabe, U.S. Patent 4,943,497.
[7] Y. Yamamoto, S. Fujita and H. Kato, PCT Int. Appl #92-20,112 (1992);
E. Masuko, Japanese Kokai Tokkyo Koho (Japanese Patent Application) JP 0535439.
[8] J.R. Dahn, R. Fong and U. von Sacken, Canadian Patent Application #2,038,631; U.S. Patent 5,264,201.
[9] J.N. Reimers and J.R. Dahn, J. Electrochem. Soc. 139 (1992) 2091.
[10] D.S. Wainwright, J. Power Sources, submitted for publication.
[11] Y. Nishikawa and T. Morita, Japanese Kokai Tokkyo Koho (Japanese Patent Application) JP 05166537 A2, JP 93166537 A2, (1993);
J. Yamamura and Y. Nishikawa, Japanese Kokai Tokkyo Koho (Japanese Patent Application) JP 05151995 A2, JP 93151995 A2 (1993).
[12] J. Morales, C. Perez-Vicente and J.L. Tirado, J. Therm. Anal. 38 (1992) 295.
[13] M.G.S.R. Thomas, W.I.F. David and J.B. Goodenough, Mater. Res. Bull. 20 (1985) 1137.
[14] Wu Li, J.N. Reimers and J.R. Dahn, Phys. Rev. B46 (1992) 3236.
[15] J.N. Reimers, Wu Li and J.R. Dahn, Phys. Rev. B47 (1993) 8486.
[16] U. von Sacken, U.S. Patent 5,180,574.
[17] R. Fong, U. von Sacken and J.R. Dahn, J. Electrochem Soc. 137 (1990) 2009.
[18] Wu Li, J.N. Reimers and J.R. Dahn, Solid State Ionics 67 (1993) 123.
[19] J.C. Hunter, U.S. Patent 4,246,253.
[20] J.M. Tarascon and D. Guyomard, Electrochim. Acta 38 (1993) 1221.